LIGHT MICROSCOPY, SCANNING AND TRANSMISSION ELECTRON MICROSCOPY OF VERTEBRATE CEREBELLAR GOLGI CELLS

Orlando J. Castejón

Instituto de Investigaciones Biológias, Facultad de Medicina
Universidad del Zulia, Apartado Postal No. 526, Maracaibo, Venezuela

Abstract

The cerebellar Golgi cells of mouse, teleost fish, primate and human species have been studied by means of light and Golgi light microscopic techniques, slicing technique, ethanol-cryofracturing and freeze fracture methods for scanning electron microscopy and ultrathin sectioning for transmission electron microscopy. The Golgi cells appeared in the granular layer as polygonal, stellate, round or fusiform macroneurons surrounded by the granule cell groups. They exhibited ascending and horizontal dendrites and a short beaded axonal plexus. Scanning microscopy revealed three-dimensional neuronal geometry and smooth outer surfaces. Freeze-fracture method showed stereospatial arrangement of endoplasmic reticulum, organelles and nuclear envelope. By means of transmission electron microscopy asymmetric synaptic connections of horizontal dendrites of Golgi cells with mossy fiber rosettes at the cerebellar glomerulus and of Golgi cell axons with granule cell dendrites were identified. Golgi cell ascending dendrites exhibited short neckless spines in the molecular layer establishing asymmetric contacts with granule cell axons or parallel fibers. Shaft asymmetric axodendritic contacts between Golgi cell dendrites and climbing fibers were also found in the molecular layer.

Key Words: Light microscopy, scanning microscopy, Golgi cell, cerebellum.

Introduction

The large stellate cells of the cerebellar granule layer (or Golgi cells) have been extensively studied in light microscopy by Golgi, Retzius, Van Gehuchten, Kolliker and Ramón y Cajal by the Golgi light microscope technique (Ramón y Cajal, 1955). Further electron and light microscope studies have been carried out among others by Eccles *et al.* (1967); Mugnaini (1972); Palay and Chan-Palay (1974); Castejón and Castejón (1972); Castejón (1976); Alvarez-Otero and Anadon (1992). Some preliminary observations on conventional scanning electron microscopy of Golgi cells have been published on general studies dealing with the cytoarchitectonic arrangement and intracortical circuits of the cerebellar cortex (Castejón and Caraballo, 1980a,b; Castejón and Valero, 1980; Castejón, 1981, 1984, 1988; Castejón and Castejón, 1991; Castejón and Apkarian, 1992; Castejón, 1993; Hojo, 1994; Castejón, 1996). More recently, the Golgi cells have been related from the cytochemical point of view, to expression of proencephalin (Spruce *et al.*, 1990), calcium binding proteins (Celio, 1990) neuropeptide immunoreactivity (Yamashita *et al.*, 1990), cholinergic properties (Illing, 1990; De Lacalle *et al.*, 1993), GABAergic system (Batini, 1990; Reichenberger *et al.*, 1993; Swan *et al.*, 1994; Takayama, 1994), glutamatergic system (Ohishi *et al.*, 1993, 1994) and glycinergic synaptic input (Dieudonne, 1995).

However, until now a detailed three-dimensional study of the cerebellar Golgi cells by means of conventional and high resolution scanning electron microscopy has not been reported. In the present paper the cerebellar Golgi cells have been examined using: (a) light microscopy to study shape and neuronal geometry; (b) conventional and high resolution scanning electron microscopy to revel outer and inner surfaces of intact and fractured Golgi cells, and (c) transmission electron microscopy to explore Golgi cell's participation in the granular and molecular layers of the cerebellar cortex. A previous and careful light and electron microscope study was needed in order to appropriately interpret scanning electron images. The aim of the present paper is to provide more complete and "in depth" information on cerebellar Golgi cells of the mouse, teleost fish, primate and human species.

Material and Methods

Light microscopy of plastic embedded material (Castejón and Caraballo, 1980a).

The brains of Swiss albino mice and teleost fishes (*Arius spixii*) were removed and the cerebellar samples were fixed immediately by immersion in 4% glutaraldehyde (0.1 M phosphate buffer solution, pH 7.4) for 4-16 hours at 4°C and postfixed for 1 hour in a similarly buffered 1% osmium tetroxide solution. Samples were then dehydrated through graded concentrations of ethanol and embedded in Araldite. Thick sections (1-1.5 μm, obtained with an LKB (was at Bromma, Sweden) Pyramitome equipped with a glass knife) were stained with toluidine blue and observed with a Zeiss II Photomicroscope (Carl Zeiss, Oberkochen, Germany).

Golgi light microscopy (Castejón, 1981)

Fragments of Swiss albino mouse and teleost fish (*Arius spixii*) cerebellar cortex (5-10 mm thick) were processed according to the rapid Golgi method. Sagittal and transverse sections of the cerebellar cortex (50-70 μm thick) were observed in a Zeiss II Photomicroscope using X25 and X40 objectives.

Slicing technique for SEM (Castejón and Caraballo, 1980a)

Specimens of *Arius spixii*, weighing 30-82 g, kept in aquaria at room temperature were used. Pieces of tissue were fixed: (1) by immersion in 5% glutaraldehyde in 0.1 M phosphate buffer (pH 7.4); (2) by vascular perfusion with 4% glutaraldehyde in 0.1 M phosphate buffer solution, pH 7.4; or (3) by immersion in the Karnovsky fixative. Slices 2-3 mm thick were cut with a razor blade and fixed overnight in the same buffered fixative. After washing in buffered saline, the tissue blocks were dehydrated through graded concentrations of ethanol, dried by the critical point method with liquid CO_2, mounted on copper stubs and coated with carbon and gold-palladium. These specimens were examined in a JEOL 100B (JEOL, Akishima, Tokyo, Japan) electron microscope with ASID scanning attachment at 20 kV.

Ethanol-cryofractography applied to human cerebellum (Castejón and Caraballo, 1980b)

This technique, originally designed by Humphreys *et al*. (1975), to scan liver and kidney tissue was applied by us to study the human cerebellar cortex. The samples, 3-5 mm thick, were fixed for 2 to 16 hours in 4% glutaraldehyde-phosphate buffer solution (0.1 M, pH 7.4) dehydrated in ethanol and frozen in liquid nitrogen. The fracture was performed with a precooled razor blade and the fragments placed in ethanol at room temperature for thawing. The critical point drying was done with liquid CO_2 followed by a coating of carbon or gold-palladium in a JEOL-46 high vacuum evaporator. The tissue was observed with a JEM 100B EM-ASID.

Freeze-fracture SEM method (Castejón, 1981)

This method was applied to study the cerebellar cortex of two teleost fishes: *Arius spixii* and Salmo trout. After Karnovsky fixation, cerebellar slices (2-3 mm thick) were cut with a razor blade and fixed by immersion in the same fixative for 4-5 hours. After washing in buffered saline, they were postfixed in 1% osmium tetroxide in 0.1 M phosphate buffer solution (pH 7.4) for 1 hour. After rinsing in a similar buffer, tissue blocks were dehydrated through graded concentrations of ethanol, rapidly frozen by plunging into Freon 22 cooled by liquid nitrogen (Haggis and Phipps-Todd, 1977) and fractured with a precooled razor blade. The fracture fragments were returned to fresh absolute ethanol for thawing. According to Haggis and Phipps-Todd (1977), in the FDFf method, the cytoplasmic and nuclear soluble proteins are washed out, presumable during the thawing step, leaving unfractured cavities surrounding the cytomembranes and allowing visualization of the surface details of cytoplasmic and nuclear structures. The tissues ware then dried by the critical point method with liquid CO_2 and coated with gold-palladium. Specimens were examined in a JEOL 100B EM-ASID scanning attachment at 80 kV.

Transmission electron microscopy (Castejón and Caraballo, 1980b)

For transmission electron microscopy (TEM), slices 1-2 mm thick of fish and mouse cerebellar cortex were immediately fixed by immersion in 4% glutaraldehyde in 0.1 M phosphate buffer solution (pH 7.4) for 4-16 hours at 4°C; or by vascular perfusion with glutaraldehyde-Alcian blue mixture in a similar buffer solution. They were postfixed for 1 hour in a similarly buffered 1% osmium tetroxide solution, dehydrated through graded concentrations of ethanol and embedded in Araldite. Thin sections were stained with uranyl and lead salts and observed with a Siemens Elmiskop I (Siemens, Berlin, Germany) or a JEOL 100B electron microscope.

Fixation of primate cerebellum for HRSEM (Castejón and Apkarian, 1992)

Upon intracardiac cannulation of juvenile rhesus monkeys the cerebellar cortex was flushed with Ringer lactate buffer and then perfusion-fixed with 4% paraformaldehyde and 0.1% glutaraldehyde in 0.05% phosphate buffer (pH 7.4). Prior to excision a perfusion with 5% buffered sucrose cleared all upper body vasculature.

Excised rhesus cerebellar cortex was minced into 2 mm³ pieces and further fixed in 2.5% electron microscopy (EM) grade glutaraldehyde in 0.1 M cacodylate buffer (pH 7.4) overnight in order to provide complete intracellular proteinaceous cross-linking. Cacodylate buffer (pH 7.4) was used to completely remove the primary fixative by rinsing the tissue several times under gentle agitation.
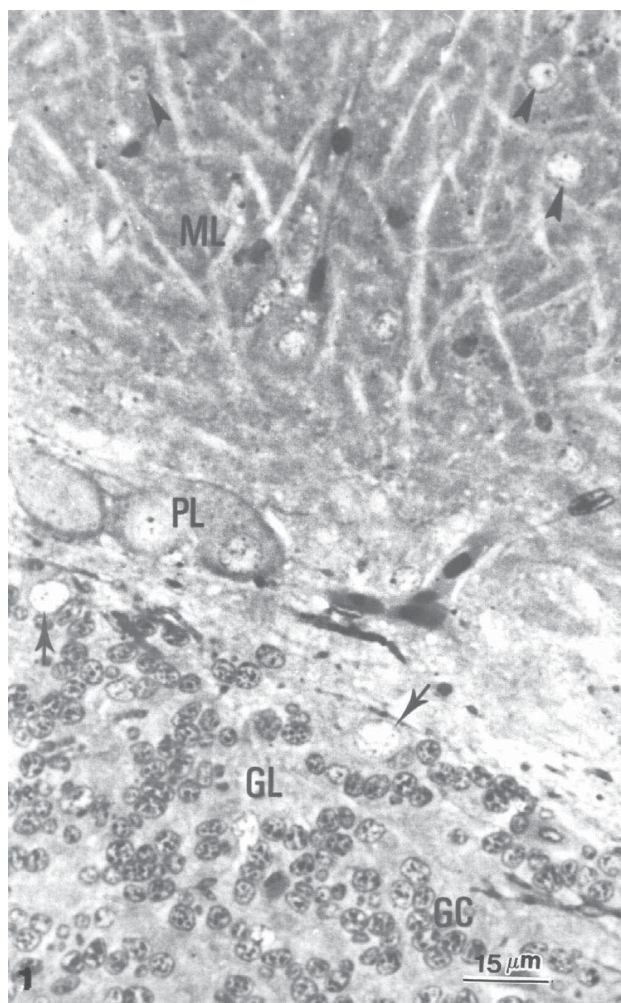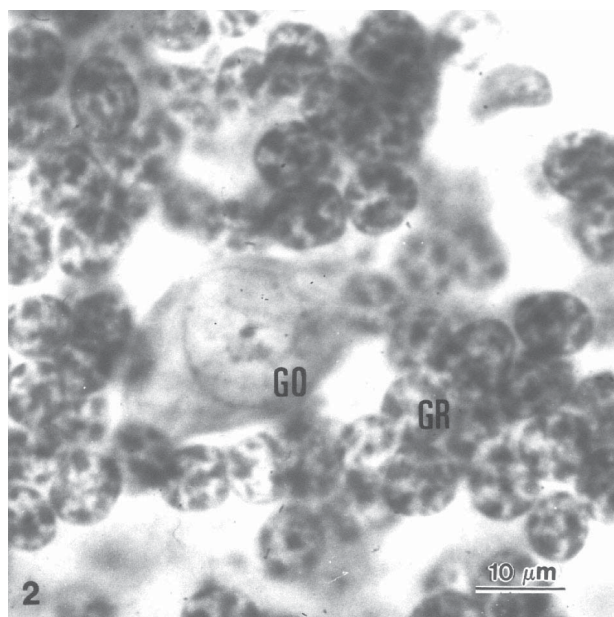
Figure 2. Photomicrograph of mouse cerebellar granular layer showing the Golgi cell (GO) as a macroneuron intercalated between the microneurons composing the granule cell groups (GR). Alcian blue staining.

Figure 1. Photomicograph of teleost fish cerebellar cortex showing the granular (GL), Purkinje (PL) and molecular (ML) layers. The Golgi cells (arrows) are observed in the granular layer surrounded by the granule cell groups. Stellate neurons (arrowheads) are seen in the molecular layer. Toluidine blue staining.

Postfixation of phospholipid moieties was accomplished by immersion in 1% OsO_4 in 0.1 M cacodylate buffer (pH 7.4) for one hour and then rinsed in cacodylate buffer several times.

Delicate specimen preparation

A graded series of ethanols (30, 50, 70, 80, 90 2x100%) was used to substitute tissue fluids prior to wrapping individual tissue pieces in preformed absolute ethanol filled parafilm cryofracture packets. Rapid freezing of packets was performed by plunging into Freon-22 at its melting point (-155°C) and then storing in LN_2. A modified tissue chopper (Sorval TC-2) equipped with a LN_2 copper stage and a precooled fracture blade (-199°C) was utilized for cryofracture. First, the packet was transferred from the LN_2 storage vessel with LN_2 chilled forceps in order to avoid thermal damage. Secondly, the cooled fracture blade was removed from the LN_2, the packet was orientated under the blade, and the arm was immediately activated to strike only the top of the packet (Apkarian and Curtis, 1986). Fractured tissue fragments were transferred into chilled absolute ethanol (4°C) and thawed. Tissues were loaded into fresh absolute ethanol filled mesh baskets within the boat of a Polaron E-3000 critical point dryer. The boat was then loaded into the dryer, and exchange with CO_2 gas at a rate of 1.2 1/min. The CPD chamber was then thermally regulated to the critical temperature and pressured at a rate of 1°C/min. Following the phase transition, the CO_2 gas was released at a gas flow rate of 1.2 l/min. (Peters, 1980). Dried specimens, shiny face up, were mounted onto aluminum stubs 9 mm x 2 mm x 1 mm for the ISI DS-130 SEM with silver paste and degassed at 5 x 10^{-7} torr prior to coating.

Metal coating for HRSEM imaging

Dried and mounted specimens were chromium coated with a continuous 2 nm film in a Denton DV-602 (Denton Vacuum, Inc., Moorestown, NJ, USA) turbo pumped sputter deposition system operated in a vacuum of Argon at 5 x 10^{-3} torr (Apkarian, 1994).

High resolution scanning electron microscopy (SEM)

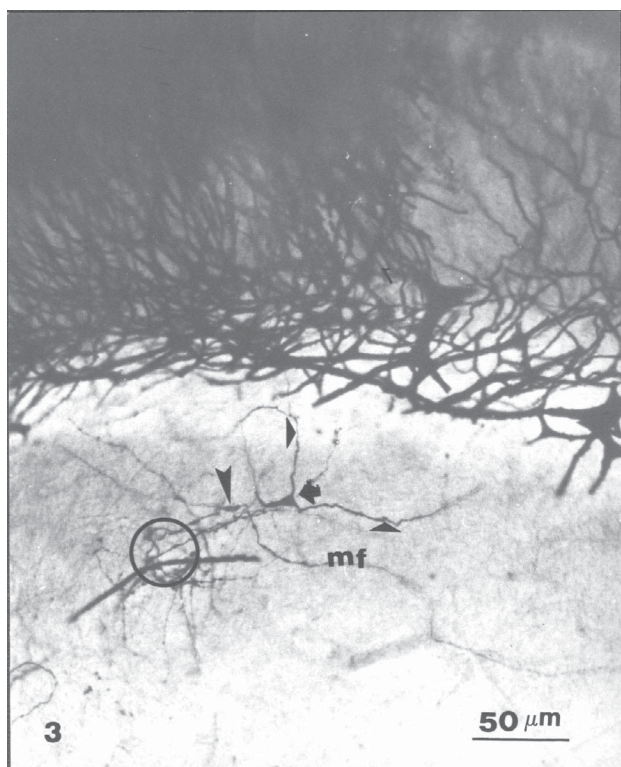Specimens were introduced onto the condenser/objective

389

Figure 3. Photomicrograph of teleost fish cerebellar cortex granular layer showing a triangular shaped Golgi cell (short arrow). The Golgi technique clearly depicted the ascending and horizontal dendrites (triangles) and the distribution area of the short axonal collateralization of Golgi cell axon within the granular layer (circled area). An afferent mossy fiber (mf) is seen bearing the mossy rosette expansion (arrowhead), in the immediate neighborhood of the Golgi cell soma.

(C/O) lens stages (predominantly primary beam generated secondary electron, SE-I, signal mode operation) of either an ISI DS-130 equipped with LaB_6 emitter or a Hitachi S-900 SE (Hitachi Limited, Tokyo, Japan) equipped with a cold cathode field emitter. Both instruments were operated at accelerating voltages of 25-30 kV in order to produce minimal spot size and adequate signal to noise ratio at all magnifications. Micrographs were soft focus printed to reduce instrumental noise (Peters, 1985).

Results

Light microscopy

Examination of plastic embedded thick sections of mouse and teleost fish cerebellum, stained by toluidine blue and Alcian blue, showed Golgi cells as large macroneurons dispersed in the granular layer and surrounded by granule cell groups (Figs. 1 and 2). They characteristically exhibited a clear cytoplasm and a vesicular nucleus. Simply counting
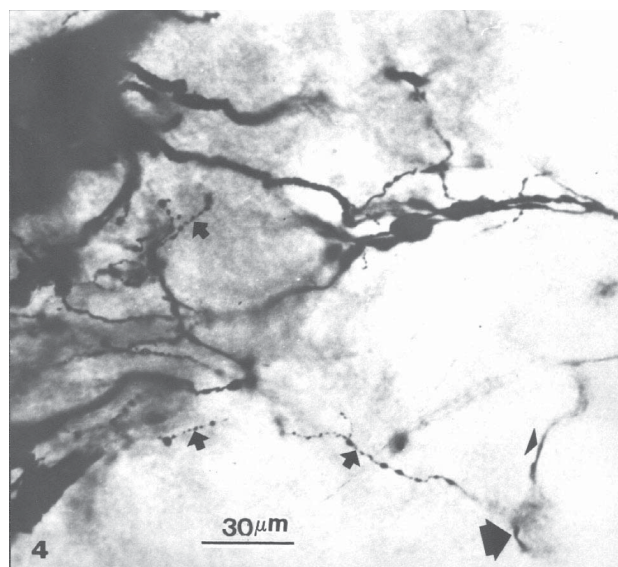

Figure 4. Photomicrograph of the beaded axonal ramifications of Golgi cell in the granular layer as seen by the Golgi technique. The Golgi cell soma (thick arrow) is partially seen in the lower right corner of the figure. The Golgi technique revealed the ascending dendrite (triangle) and the axonal collaterals (thin arrows).
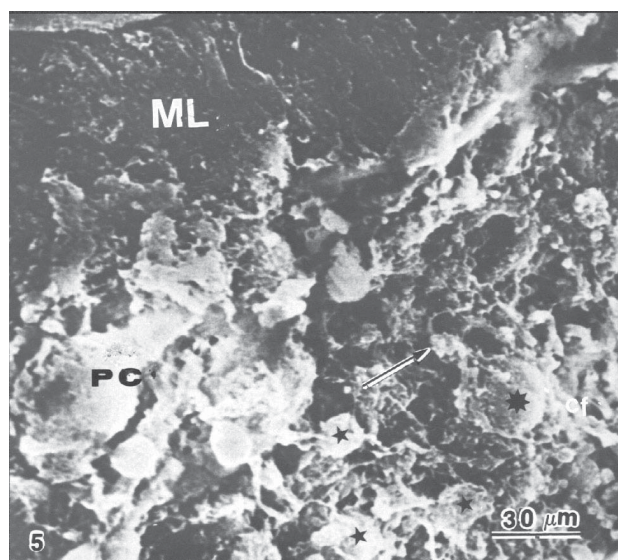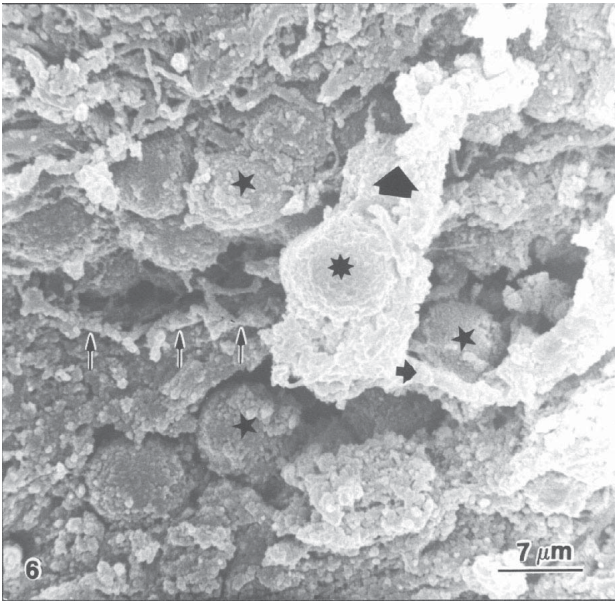

Figure 5. Scanning electron micrograph of teleost fish cerebellar cortex. Gold-palladium coating. The exposed surface of the granular layer by means of the slicing technique showed a Golgi cell soma (asterisk) surroun-ded by granule cell bodies (stars). An afferent climbing fiber (CF) is observed approaching the Golgi cell soma. In addition, a mossy fiber (arrow) and its mossy rosette is also seen. In the left side of the figure, a Purkinje cell body (PC) is present. The molecular layer (ML) is seen undifferentiated at the top of the figure.

Figure 6. Scanning electron micrograph of the human cerebellar granular layer. Gold-palladium coating. The ethanol-cryofracturing technique exposed the round Golgi cell soma (asterisk), the ascending dendrite toward the molecular layer (thick arrow), and the horizontal dendrite (thin arrow) and Golgi axonal plexus (large arrows) in the granular layer. The granule cell bodies (stars) are observed surrounding the Golgi cell.
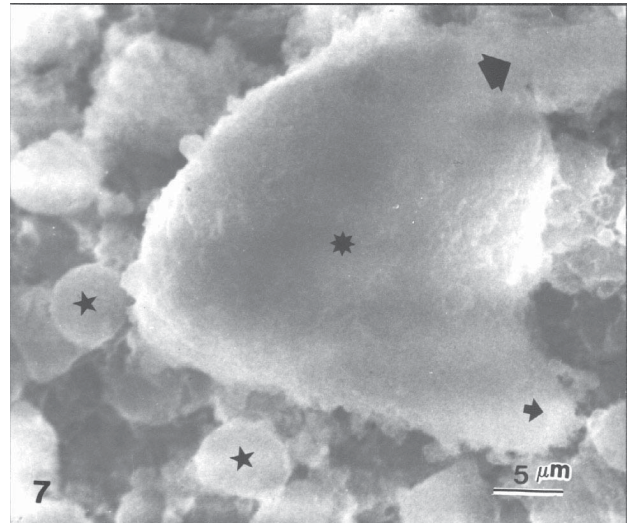

Figure 7. Scanning electron micrograph of primate cerebellar cortex. Chromium coating. Unfractured Golgi cell soma (asterisk) exposed by the cryofracture technique exhibiting a round shape, smooth surface and the site of emergency of horizontal (thin arrow) and ascending dendrites (thick arrow). The granule cells (stars) surround the Golgi cell.

the granule cells surrounding the Golgi cells, the Golgi cell-granule cell ratio was 1: 15 in the teleost fish cerebellum and 1:30 in the mouse cerebellar cortex. Some Golgi cells were observed at certain distances below the Purkinje cell layer and others in close proximity to the glomerular regions. They may be polygonal, stellate, round or fusiform in shape. The cell bodies varied from 10 μm to 25 μm in maximal dimension.

The Golgi light microscope technique showed that the Golgi cell of mouse and teleost fished exhibited ascending and horizontal dendrites and an axonal arborization dispersed in the granular layer (Fig. 3), supporting former classical descriptions of these cells. At higher magnification the axonal plexus of Golgi cells showed a typical beaded shape (Fig. 4).

Scanning electron microscopy of unfractured Golgi cells.

Low magnification examination of teleost fish cerebellar cortex, processed according to the slicing technique and coated with gold-palladium, displayed the three-dimensional view of the round Golgi cell soma in the granular layer. The afferent mossy and climbing fibers were seen approaching to the cell soma, which appear surrounded
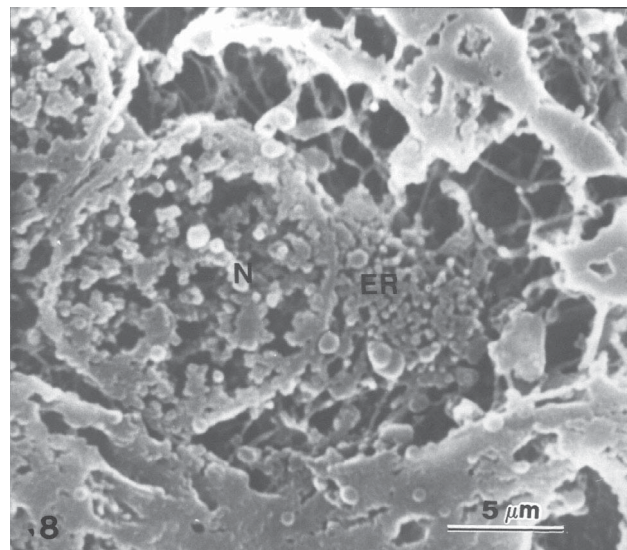

Figure 8. Scanning electron micrograph of teleost fish cerebellar cortex. Gold-palladium coating. The freeze-fracture method for SEM disclosed the outer surface of endoplasmic reticulum (ER) of Golgi cell soma, extended between the nuclear envelope and the plasma membrane. The fractured nucleus (N) displays the chromatin masses. The cytoplasmic matrix has been washed out exposing the inner cytoplasmic details and cell organelles.
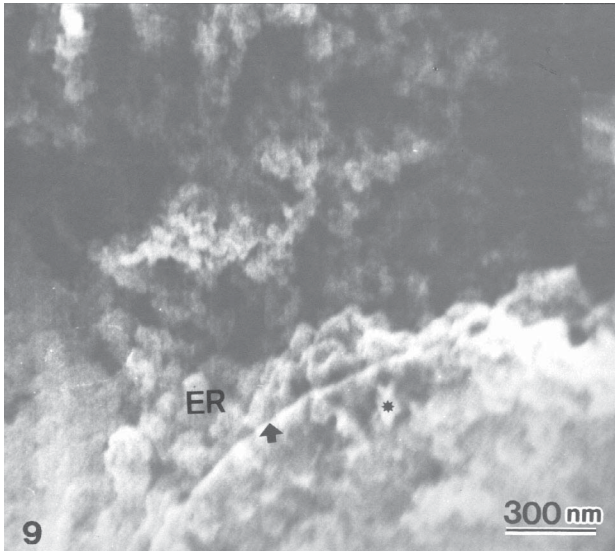
Figure 9. High resolution scanning electron micrograph of primate cerebellar cortex. Chromium coating. The fractured Golgi cell exhibits the outer surface of perinuclear endoplasmic reticulum (ER), the SE-1 density profile of the nuclear envelope (arrow) and the high mass density of peripheral heterochromatin masses (asterisk).

by the granule cells (Fig. 5).

Exploring the granular layer of human cerebellar cortex, processed according with the ethanol-cryofracturing technique and coated with gold-palladium, we found that the image of the large Golgi cells was similar to that obtained with the Golgi light microscopy technique. The cryofracture process with liquid nitrogen (slow freezing) exposed not only the cell body but in addition the dendritic and axonal ramifications (Fig. 6). The depth of focus of the scanning electron microscope allows us to trace the horizontal dendrites and the axonal ramifications pervading the neighboring neuropil of the granular layer and the ascending dendrites directed toward the molecular layer. The fracture process limited the observation of the synaptic connections with the afferent fibers and neighboring granule cells. Dark and wide spaces were observed surrounding the Golgi cells and the granule cells, due to a selective removal of neighboring neuroglial cells during the cryofracturing process. This useful artifact facilitated the visualization of the hidden outer surface of Golgi cells.

Examination of the outer surface of Golgi cells in primate cerebellar cortex, processed according to delicate handling for high resolution scanning electron microscopy and coated with a 2 nm chromium film, showed the smooth true outer surface of Golgi cells and the sites of emergence of their processes (Fig. 7).
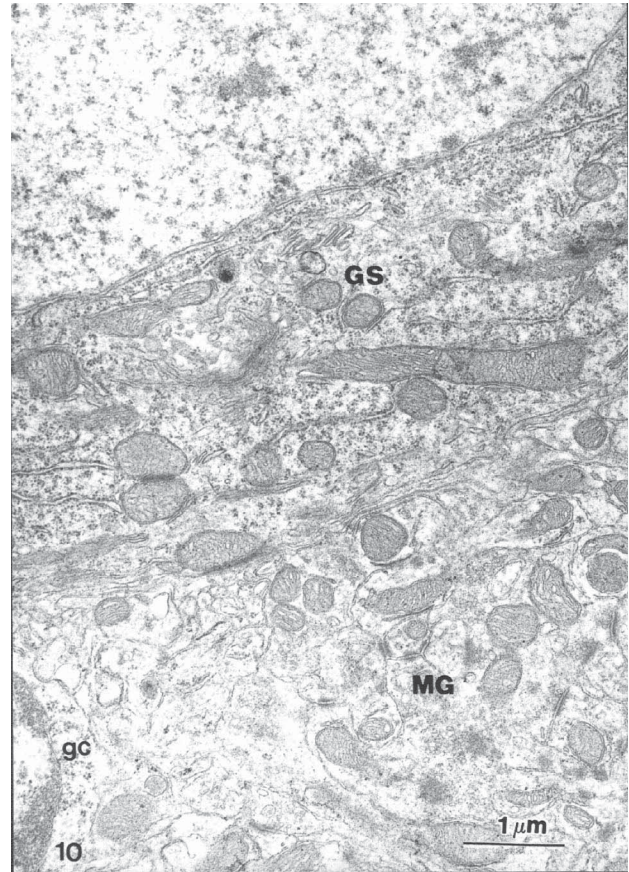

Figure 10. Transmission electron micrograph of mouse cerebellar cortex. The Golgi cell soma (GS) appears located in the vicinity of a mossy glomerulus (MG) and a granule cell (GC).

Scanning electron microscopy of fractured Golgi cells.

The freeze-fracture method for SEM, using Freon 22 cooled by liquid nitrogen (fast freezing) and applied to the study of teleost fish cerebellum, revealed at low magnification the fractured Golgi and granule cells. The three-dimensional arrangement and the inner details of the fractured cytoplasm and nucleus were observed. The outer surface and stereospatial arrangement of the Golgi cell rough endoplasmic reticulum and cellular organelles and also the chromatin substance within the cell nucleus were seen (Fig. 8). In this case, the cryofracture method and the washing out process of the soluble fraction of the cytoplasm or cytosol during the thawing step made possible the visualization of the outer surface of cytomembranes.

Using the freeze-fracture method for SEM applied to the primate cerebellar cortex and processing for high resolution scanning electron microscopy, in samples coated with chromium (2 nm thick), it was possible to observe the outer surface of perinuclear rough endoplasmic reticulum,

Figure 11. Transmission electron micrograph of mouse cerebellar cortex granular layer at the level of mossy glomerular region. The Golgi cell axonic ending (GA) appears as a small profile at the glomerular peripheral region making asymmetric synaptic contact (arrow) with the granule cell dendrite. The mossy rosette fiber (mf) appears at the lower left corner of the figure as a giant expansion containing spheroidal synaptic vesicles and making also asymmetric synaptic contacts with the granule cell dendrites. Note that the Golgi axonic ending is a small synaptic knob containing flattened or oval synaptic vesicles. The profiles of the Golgi axonic ending and the mossy rosette fiber were labeled with black ink to show the different shape, size and location in the glomerular region.

nuclear envelope and heterochromatin masses of Golgi cells (Fig. 9).

Transmission electron microscopy (TEM)

Due to the limited resolving power of conventional scanning electron microscopy we used TEM in order to study the synaptic relationships of Golgi cells in the granular and molecular layers. Ultrathin sections of glutaraldehyde-osmium fixed mouse cerebellar cortex were observed in order to explore the participation of the Golgi cell in the formation of mossy glomerular islands. Golgi cells located in the immediate vicinity of mossy glomerulus were studied (Fig. 10). The Golgi cell showed the typical structure of a macroneuron, with well developed rough endoplasmic reticulum, mitochondria, Golgi complex, lysosomes and multivesicular bodies.

The Golgi cell axonal endings were seen at the periphery of the glomerular region as round or longitudinal profiles located between the granule cell bodies and the granule cell dendritic processes and surrounding the central mossy rosette fiber. They contained a small, mixed population of loosely dispersed, flattened, ellipsoidal and spheroidal synaptic vesicles and established asymmetric synaptic contacts with the granule cell dendrites (Fig. 11). The Golgi axonic endings appeared as small synaptic endings in comparison with the large mossy fiber rosette expansions located at the center of the glomerular region. The mossy rosette in addition contained a hugh population of synaptic vesicle formed by hundreds of spheroidal synaptic vesicles.

In teleost fishes, the Golgi axonal endings were observed in cryofractured samples. Fractured surfaces passing tangential to the granule cell soma showed beaded axonal endings of Golgi cells making 1 to 1 axodendritic contacts with granule cell dendritic claws (Fig. 12).

The Golgi cell horizontal dendrites appeared larger and more electron dense than the granule cell dendrites,
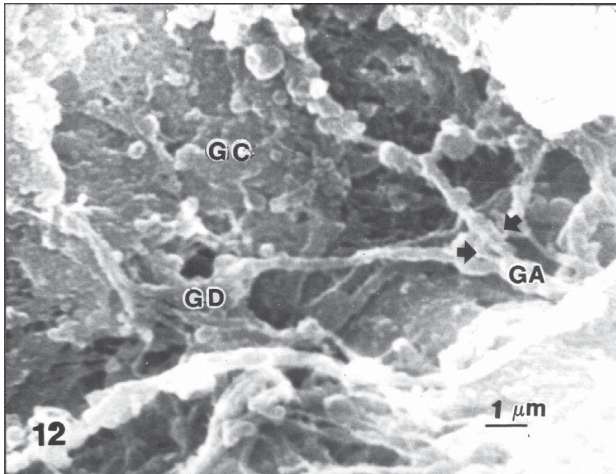
Figure 12. Scanning electron micrograph of teleost fish cerebellar cortex showing the synaptic relationship between the beaded shaped Golgi cell axonic ending (GA) and the granule cell dendrite (GD). The outer surface of the granule cell (GC) is observed at the upper left corner of the figure. The arrows point out the site of synaptic relationship.

———————————

containing numerous mitochondria and clusters of free ribosomes. They were traced to the center of the mossy glomerular region (Fig. 13), where they established asymmetrical synaptic contacts with mossy fiber rosettes. The dendritic tip of the Golgi cell making contact with the mossy fiber rosette did not show the typical dendritic claw that characterizes granule cell dendrites surrounding the mossy rosettes. The Golgi dendrites participating in the formation of mossy glomerulus exhibited dendro-dendritic junctions with the neighboring, clear, granule cell dendritic profiles. In mouse cerebellar cortex, fixed and stained simultaneously by vascular perfusion with a glutaraldehyde-Alcian blue mixture, the Golgi horizontal dendrites appeared darkly stained, whereas the granule cell dendrites remained unstained. This differential staining property facilitated the identification of Golgi dendrites at the glomerular region (Fig. 14).

The somatic surface of Golgi cells was explored in mouse, teleost fish, primate and human. Synapses "in marron", as described by Chan-Palay and Palay (1971), have not been observed thus far. Some isolated, small, axosomatic synaptic endings containing flattened vesicles were observed intimately applied to the Golgi cell plasma membrane (Fig. 15). However, pre- and post-synaptic membrane specializations characteristic of axo-somatic synapses were not observed. This synaptic knob possibly corresponded to the terminal ending of a Purkinje cell recurrent axonal collateral.

At the level of the molecular layer, the Golgi cell ascending dendrites were characterized as clear dendritic profiles provided with short, neckless spines. These spines look like gemmules and formed axospiny synaptic contacts with parallel fibers or granule cell axons (Fig. 16). The Golgi cell dendritic shaft also showed extensive axodendritic asymmetric contacts with the climbing fiber terminals. These latter appeared remarkably larger compared with the parallel fiber endings. Similar axo-dendritic contacts of climbing fibers with Purkinje cell dendrites were also observed in the molecular layer (Fig. 17). The Purkinje cell dendrites were clearly differentiated from Golgi cell dendrites by the presence of lamellar cisterns, which were absent in the Golgi cell dendrites.

Discussion

Previous light and electron microscopic studies of cerebellar Golgi cells have reported their basic structural features (For a detailed review, see Palay and Chan-Palay, 1974). In the present study we have correlated these features with scanning electron microscope images in order to compare them properly with Golgi cell neuronal geometry and synaptic connections. In our investigation, a previous light microscopic study was required in order to orientate the position of the cerebellar folia during the trimming process and to assure that sagittal and transverse sections of the cerebellar cortex were obtained. In addition, during the specimen mounting and orientation on specimen stubs it was essential to observe the cut surface (slicing technique) or the fracture surface (cryofracture method) under a stereoscopic microscope. Orienting the tissue fragments according to the position required (sagittal, transverse or tangential planes) is also fundamental, as a previous step to metal deposition either by gold-palladium or chromium coating (Castejón, 1993).

The previous Golgi light microscopic study is also basically important for a rational and adequate interpretation of transmission and scanning electron microscope images of Golgi cell intracortical circuits. Scanning electron microscope images showed better resolution, depth of focus, and mass density than the Golgi light microscope images, but only within the restricted field of the cut section or the fracture surface obtained. The Golgi light microscope technique offers the advantage of a larger panoramic view for tracing intracortical circuits. In this context both techniques should be complementary to each other for correlative purposes. The t-butyl alcohol freeze drying device applied to the study of human cerebellar cortex has also disclosed the Golgi cells in the granular layer (Hojo, 1994).

An advantage of the scanning electron microscope study of the granular layer is that granule cells, Golgi cells, afferent fibers (mossy and climbing fibers) and glomerular
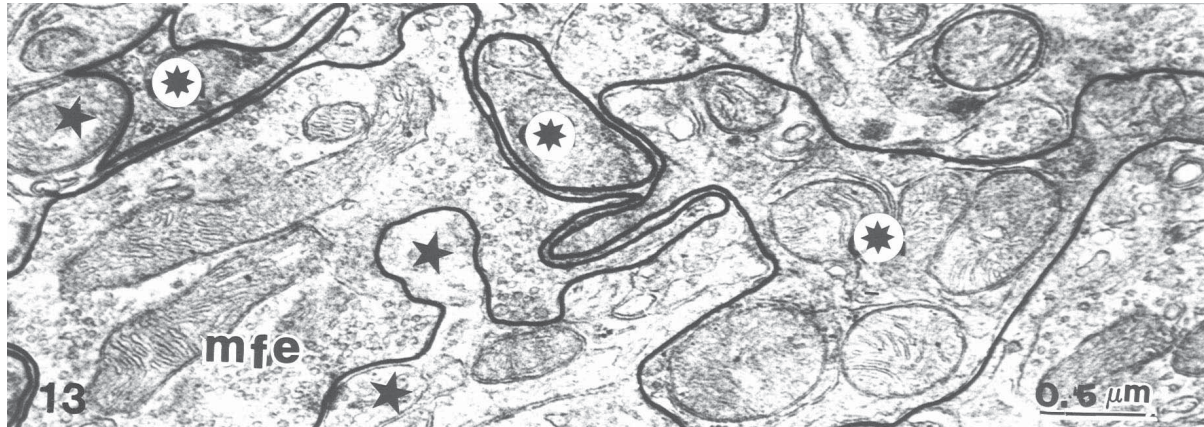
Figure 13. Transmission electron micrograh of mouse cerebellar cortex showing the dense Golgi horizontal dendrites (asterisks) making asymmetric synaptic contact with the mossy fiber ending (mfe). The clear granule cell postsynaptic dendritic endings have been labeled with stars. The axonal and dendritic profiles have been traced with India ink to outline the composition of the glomerular region.
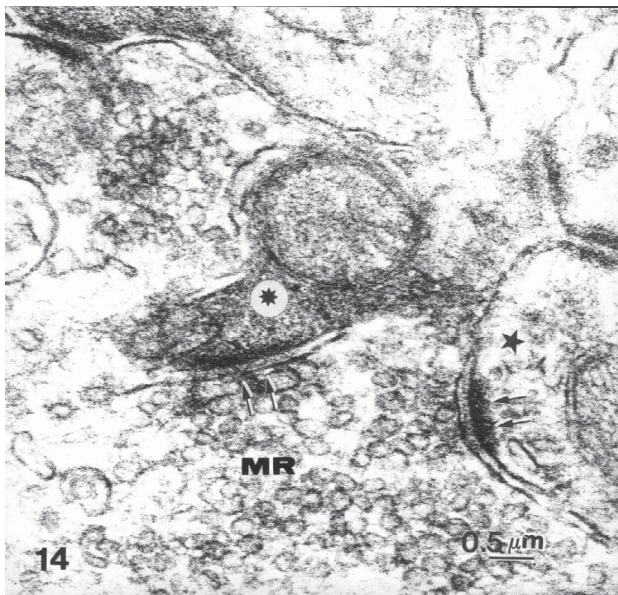

Figure 14. Transmission electron micrograph of mouse cerebellar cortex perfused with a mixture of glutaraldehyde-Alcian blue solution. The Golgi dendrite (asterisk) appears densely stained whereas the granule dendrite (star) remains clear. Both types of dendritic profiles establish asymmetrical synaptic contacts (arrows) with the mossy fiber rosette (MR).

Figure 15. Transmission electron micrograph of mouse cerebellar cortex showing an axosomatic presynaptic ending intimately applied to the Golgi cell (Go) plasma membrane. Pre- and post-synaptic membrane specializations are not distinguished. The presynaptic ending showed predominantly flattened synaptic vesicles and possibly correspond to a Purkinje cell recurrent collateral axonic ending (PR). A Golgi apparatus (GA) is observed in sub lemmal and subsynaptic localization.

regions can be simultaneously visualized. This panoramic view, as illustrated in Figure 5, could not be obtained with separate light microscopic or electron microscopic observations.

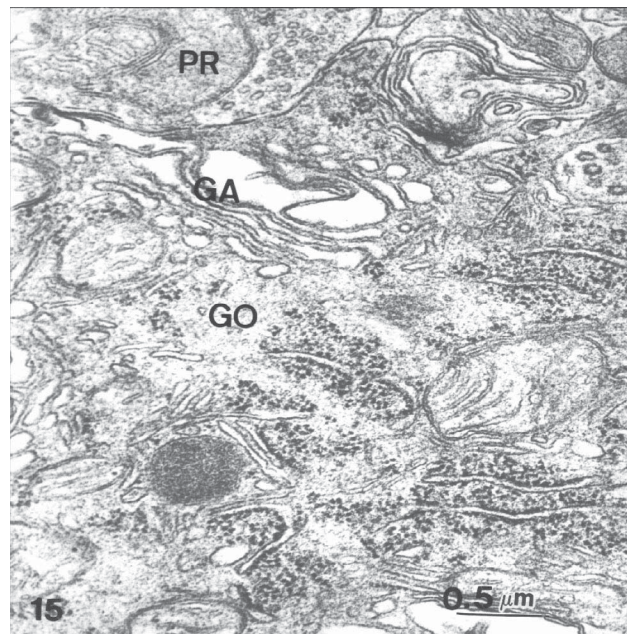The cryofracture method, either by slow or fast freezing, exposed the hidden surfaces of Golgi cells, par-

tially ensheathed by the neuroglial cells of the granular layer. The fractographs randomly obtained permit tracing of the processes of Golgi cells, as depicted in Figure 6. In this
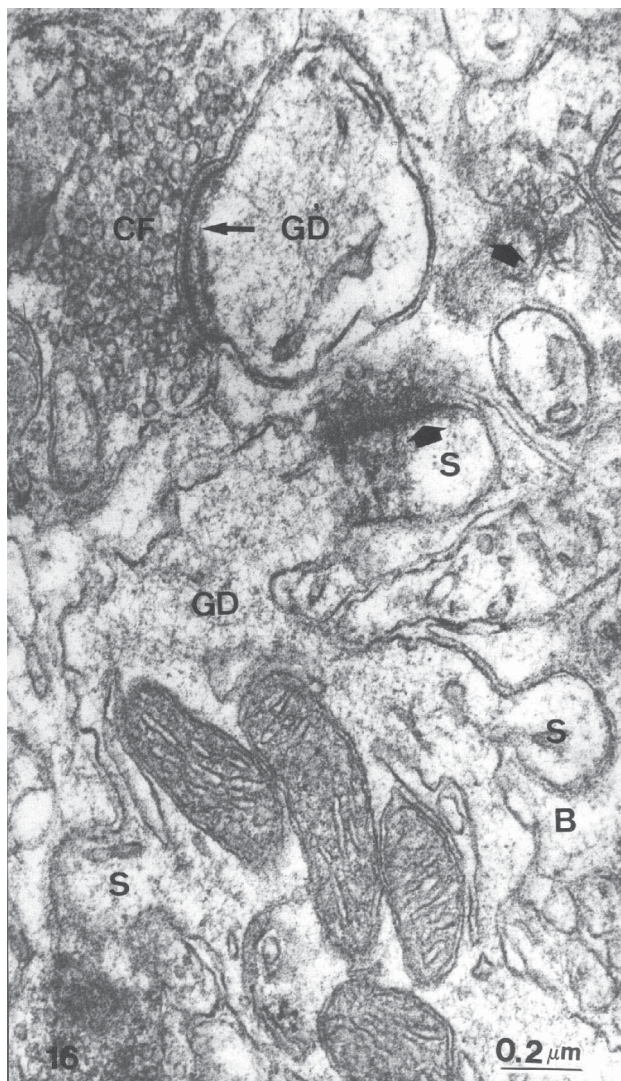
Figure 16. Transmission electron micrograph of mouse cerebellar molecular layer. A clear Golgi cell ascending dendrite (GD) is observed exhibiting short, neckless spines (S). A large axodendritic asymmetric synaptic contact (arrow) between a climbing fiber ending (CF) and the Golgi ascending dendrite is observed. The short arrows indicate the spine synaptic relationship between the parallel fiber or granule cell axon and the Golgi cell dendritic spines. The Bergmann glial cell cytoplasm (B) appears ensheathing the synaptic contacts.

Figure 17. Transmission electron micrograph of mouse cerebellar molecular layer. A climbing fiber ending (CF) makes axodendritic contact with a Purkinje cell dendrite (PD). Note that the Purkinje cell dendrites exhibit lamellar cisterns (LC), which are absent in the Golgi cell dendrites as shown in the previous figure.

---

case the gold-palladium coating, which generates type II and III signals, offers the advantage of high surface contrast and topographic information for tracing neuronal processes and intrinsic cortical circuits (Castejón, 1996). The use of chromium coating, 2 nm thick, for high resolution scanning electron microscopy, as shown in Figures 7 and 9, offers the additional advantage of studying (at higher magnifications) the neuronal outer surface in unfractured cells and the inner
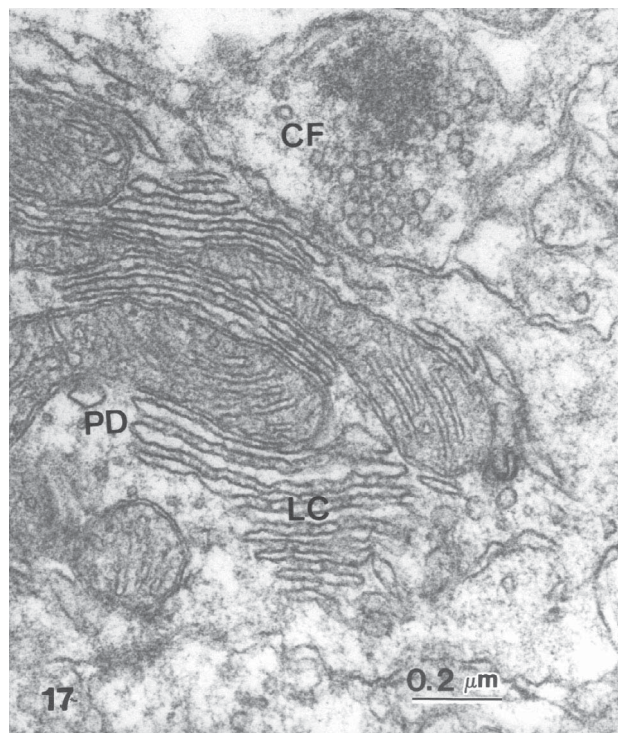
three-dimensional organization of the fractured nerve cells.

With the freeze-fracture method for SEM the nuclear and cytoplasmic details of Golgi cells could be explored. According to Haggis and Phipps-Todd (1977), during the freeze-fracture method the cytoplasmic and nuclear soluble proteins are washed out, presumably during the thawing step. This leaves fracture cavities surrounding the cytomembranes and allows visualization of the surface details of cytoplasmic and nuclear structures. The freeze-fracture method provided a view of the stereo-spatial configuration of rough endoplasmic reticulum, nuclear envelope and chromatin arrangement of Golgi cells.

Transmission electron microscopy, by means of ultrathin sections, remains until now the most suitable technique for tracing Golgi cell processes in the granular and molecular layer and for identifying the synaptic connections with afferent fibers (climbing fibers and mossy fiber). It also reveals intrinsic neuronal cell processes. In this connection, our study supports and extends previous transmission electron microscopic studies (Fox *et al.*, 1962, 1967; Szentagothai, 1964; Larramendi, 1968; Hillman, 1969; Hamori and Szentagothai, 1966; Sotelo, 1969; Uchizono, 1969;

Castejón, 1971; Palay and Chan-Palay, 1974; Castejón and Apkarian, 1992).

More recently, further studies have been carried out in our laboratory to study the outer and inner surface of cerebellar synaptic junctions (Castejón, 1996), so as to provide the potential contribution of high resolution scanning electron microscopy in the study of cerebellar synaptic relationships.

Acknowledgements

References

Alvarez-Otero R, Anadon R (1992). Golgi cells of the cerebellum of the dogfish, Scyliorhinus canicula (elasmobranch): A Golgi and ultrastructural study. J Hirnforsch **33**, 321-327.

Apkarian RP, Curtis JC (1986) Hormonal regulation of capillary fenestrae in the rat adrenal cortex: Quantitative studies using objective lens staging scanning electron microscopy. Scanning Electron Microsc 1986; IV, 1381-1393.

Apkarian RP (1994) Analysis of high quality mono-atomic chromium films used in biological high resolution scanning electron microscopy. Scanning Microsc **8**, 1994.

Batini C (1990) Cerebellar localization and colocalization of GABA and calcium binding proteins - D28K. Arch Ital Biol **128**, 127-149.

Castejón OJ (1971) Ultrastructure of human cerebellar glomeruli. Invest Clín **38**, 49-72.

Castejón OJ, Castejón HV (1972) Light microscope, cytochemistry and ultrastructural study of mouse cerebellar Golgi cells. Rev Mic Elect **1**, 162-163.

Castejón OJ (1976) Ultrastructure of the Golgi cells of the cerebellar cortex. Bol Acad Sc Phys Mat Nat **107**, 67-110.

Castejón OJ, Valero, C (1980) Scanning electron microscopy of human cerebellar cortex. Cell Tissue Res **212**, 363-374.

Castejón OJ, Caraballo AJ (1980a) Light and scanning electron microscopy study of cerebellar cortex of teleost fishes. Cell Tissue Res **207**, 211-226.

Castejón OJ, Caraballo AJ (1980b) Application of cryofracture and SEM to the study of human cerebellar cortex. Scanning Electron Microsc. 1980; IV, 197-207.

Castejón OJ (1981) Light microscope, SEM and TEM study of fish cerebellar granule cells. Scanning Electron Microsc 1981; IV, 105-113.

Castejón OJ (1984) Low resolution scanning elec-tron microscopy of cerebellar neurons and neuroglial cells of the granular layer. Scanning Electron Microsc 1984; III, 1391-1400.

Castejón OJ (1988) Scanning electron microscopy of vertebrate cerebellar cortex. Scanning Microsc **2**, 569-597.

Castejón OJ, Castejón HV (1991) Three-dimensional morphology of cerebellar protoplasmic islands and proteoglycans content of mossy fiber glomerulus: A scanning and transmission electron microscope study. Scanning Microsc **5**, 477-494.

Castejón OJ, Apkarian RP (1992) Conventional and high resolution scanning electron microscopy of outer and inner surface features of cerebellar nerve cells. J Submicrosc Cytol Pathol **24**, 549-562.

Castejón OJ (1993) Sample preparation technique for conventional and high resolution scanning electron microscopy of the central nervous system. The cerebellum as a model. Scanning Microsc **7**, 725-740.

Castejón OJ (1996) Conventional and high resolution scanning electron microscopy of cerebellar synaptic junctions. Scanning Microsc **10**, 177-186.

Celio MR (1990) Calbindin D-28K and parvalbumin in the rat nervous system. Neuroscience **35**, 475-475.

Chan-Palay V, Palay, S (1971) The synapse "en marron" between Golgi II neurons and mossy fiber in the rat's cerebellar cortex. Z Anat Entwickl Gesch **133**: 274-287.

De Lacalle S, Hersh LB, Saper CB (1993) Cholinergic innervation of the human cerebellum. J Comp Neurol **328**, 364-376.

Dieudonne S (1995) Glycinergic synaptic currents in Golgi cells of the rat cerebellum. Proc Nat Acad Sci **92**, 1441-1445.

Eccles JC, Ito M, Szentagothai J (1967) The Cerebellum as a Neuronal Machine. Springer-Verlag, New York. pp. 1-31.

Fox CA (1962) Fine structure of the cerebellar cortex. In: Correlative Anatomy of the Nervous System. Crosby EC, Humphreys T, Lauer EW (eds.)., MacMillan Co., New York. pp 192-198.

Fox CA, Hillman DE, Siegesmund KA, Dutta CR (1967) The primate cerebellar cortex. A Golgi and electron microscopic study. Prog Brain Res **25**: 174-225.

Haggis GH, Phipps-Todd B (1977) Freeze-fracture scanning electron microscopy. J Microsc **111**, 193-201.

Hamori J, Szentagothai J (1966) Participation of Golgi neuron processes in the cerebellar glomeruli: An electron microscopic study. Exp Brain Res **2**: 35-48.

Hillman DE (1969) Neuronal organization of the cerebellar cortex in amphibia and reptilia. In: Neurobiology of Cerebellar Evolution and Development. Llinas R. (ed.). Am Med Assoc: Educ & Res Fnd, Chicago, IL. pp. 279-325.

Hojo T (1994) An experimental scanning electron mi-

croscopic study of human cerebellar cortex using the t-butil alcohol freeze-drying device. Scanning Microsc **8**, 303-313.

Humphreys WJ, Spurlock BO, Johnson JS (1975) Transmission electron microscopy of tissue prepared for scanning electron microscopy by ethanol cryofracturing. Stain Tech **50**, 119-125.

Illing RB (1990) A subtype of cerebellar Golgi cells may be cholinergic. Brain Res **9**, 267-274.

Larramendi LMH (1968) Morphological characteristics of extrinsic and intrinsic nerve terminals and their synapses in the cerebellar cortex of the mouse. In: The Cerebellum in Health and Diseases. Field WS, Willes WD (eds.)., Warren H. Green Inc., St. Louis. pp. 63-110.

Mugnaini E (1972) The histology and cytology of the cerebellar cortex. In: The Comparative Anatomy and Histology of the Cerebellum. The Human Cerebellum. Cerebellar Connections and Cerebellar Cortex. Larsell O, Jansen J (eds.)., The University of Minnesota Press, Minneapolis, MN. pp 201-251.

Ohishi H, Shigemoto R, Nakanishi S, Mizuno N (1993). Distribution of the messenger RNA for a metabotropic glutamate receptor mGlu R2, in the central nervous system of the rat. Neuroscience **53**, 1009-1018.

Ohishi H, Ogawa-Meguro R, Shigemoto R, Kaneko T, Nakanishi S, Mizuno N (1994). Immunohistochemical localization of metabotropic glutamate receptors mGluR2 and mGluR3, in rat cerebellar cortex. Neuron **13**, 55-66.

Palay SL, Chan-Palay V (1974) Methods. In: Cerebellar cortex. Cytology and Organization. Springer-Verlag, Berlin. pp 322-336.

Peters KR (1980) Improved handling of structural fragile cell-biological specimens during electron microscopic preparation by the exchange method. J Microsc **118**, 429-441.

Peters KR (1985) Noise reduction in high magnification micrographs by soft focus printing and digital image processing. Scanning **7**, 205-215.

Ramón y Cajal S (1955) Histologie du Système Nerveux de l'Hommme et des Vertèbres. (Histology of The Nervous System of Humans and Vertebrates). Vol. 2. Consejo Superior de Investigaciones Científicas, Instituto Ramón y Cajal. Madrid, Spain. pp 55-79.

Reichenberger I, Streit P, Ottersen OP, Dieringer N (1993) GABA and glycine-like immunoreactivities in the cerebellum of the frog. Neurosc Lett **154**, 89-92.

Sotelo, C (1969) Ultrastructural aspects of the cerebellar cortex of the frog. In: Neurobiology of Cerebellar Evolution and Development. Llinas R. (ed.). Am Med Ass/ Educ & Res Fnd, Chicago. pp. 327-371.

Spruce BA, Curtis R, Wilkin GP, Glower DM (1990). A neuropeptide precursor in cerebellum: Proenkephalin exist in subpopulations of neurons and astrocytes. EMBO J **9**, 1787-1795.

Swan M, Najlerahim A, Watson RE, Bennet JP (1994). Distribution of mRNA for the GABA transporter GAT-1 in the rat brain. J Anat **185**, 315-323.

Szentagothai J (1964) The use of degeneration methods in the investigation of short neuronal connections. Prog Brain Res **14**, 1-32.

Takayama C (1994) Altered distribution of inhibitory synaptic terminals in reeler cerebellum with special reference to malposition of GABAergic neurons. Neurosci Res **20**, 239-250.

Uchizono K (1969) Synaptic organization of the mammalian cerebellum. In: Neurobiology of Cerebellar Evolution and Development, Llinas R. (ed.). Am Med Ass/ Educ & Res Fnd, Chicago. pp. 548-583.

Yamashita A, Hayashi M, Shimuzu K, Oshima K (1990) Neuropeptide-immunoreactive cells and fibers in the developing primate cerebellum. Brain Res Dev **51**, 19-25.

Discussion with Reviewers

A. Kittel: Are similarities and differences of the Golgi Network in the chosen species?

Author: At the present time, we cannot establish differences of Golgi cell connections in the species examined. Basically they share a common Golgi cell morphological pattern. We have studied different vertebrate species as part of systematic study of cerebellar cortex carried out in our laboratory from the structural and cytochemical point of view. We have applied light and electron microscopy to the study of mouse, rat, teleost fish, primate and human in order to study the evolution of cerebellar nerve cell types, organization, synaptic connections and formation of intracortical circuits.

T. Hojo: You described that the Golgi light microscope technique offers the advantage of a large panoramic view for tracing intracortical circuits. In this context both techniques (Scanning microscope and Golgi light microscopic study) should be complementary used for correlative purposes. As you know in my study (Hojo, 1994), we have presented a figure which had a large panoramic view for tracing Golgi cell intracortical circuits around Purkinje cell in the human cerebellar cortex using the t-butyl alcohol freeze-drying device.

Author: This is an interesting observation. The possibility for tracing intracortical circuits (see, Castejón *et al*., 1994) with conventional and high resolution SEM is mainly due to a selective removal of the neuroglial cells ensheathing the nerve cells, which occurs during the sample preparation procedures. Apparently the neuroglial cells behave as weak tissue resistant pathways. During the cryofracture process the clivage plane follows the neuroglial ensheathment of nerve cells.

Additional References

Castejón OJ, Castejón HV, Apkarian RP (1994) High resolution (SE-I) scanning electron microscopy features of primate cerebellar cerebellar cortex. Cell Mol Biol **40**, 1173-1180.